A slave-boson approach to ferromagnetism in the large-U Hubbard model



1993 J. Phys.: Condens. Matter 5 4847

(http://iopscience.iop.org/0953-8984/5/27/029)

J. Phys.: Condens. Matter 5 (1993) 4847–4854. Printed in the UK

# A slave-boson approach to ferromagnetism in the large-$U$ Hubbard model

Burkhard Möller, Klaus Doll† and Raymond Frésard

Institut für Theorie der Kondensierten Materie, Universität Karlsruhe, Physikhochhaus, 7500 Karlsruhe, Federal Republic of Germany

Received 7 December 1992, in final form 19 April 1993

**Abstract.** We determine the ground-state phase diagram of the Hubbard model on the square lattice allowing for homogeneous spiral, antiferromagnetic, ferromagnetic and paramagnetic phases in the overall parameter range. This is obtained from a saddle-point approximation of a spin-rotation-invariant form of the slave-boson representation introduced by Kotliar and Ruckenstein. In addition we determine analytically the transition point for infinite repulsive interaction strength between the Nagaoka state and the paramagnetic state on any bipartite lattice.

## 1. Introduction

Originally introduced in order to describe magnetism in transition metals, the Hubbard model has been most intensively investigated since Anderson's proposal [1] that the model should capture the essential physics of the cuprate superconductors. From earlier attempts to obtain the magnetic phase diagram (for an overview see the book by Mattis [2]) one can deduce that ferromagnetic and antiferromagnetic orders compete for strong repulsive interaction strength and moderate hole doping, the former being stabilized for a very small amount of holes in the half-filled band, whereas the latter is preferred at half filling. More recent calculations [3] established that the ground state of the Hubbard model on the square lattice shows long-ranged antiferromagnetic order, with a charge excitation gap. However, the problem of mobile holes in an otherwise antiferromagnetic background remains mostly unsolved, and even the stability of the Nagaoka state has been questioned [4]. Suggestions for a very wide ferromagnetic domain in the phase diagram based on the restricted Hartree–Fock approximation have been made by several authors on the cubic lattice [5], and on the square lattice [6–10]. However, this domain appears for large interaction strength where the Hartree–Fock approximation ceases to be controlled, as for small $U$ the paramagnetic state is seen to be unstable towards an incommensurate spin order at a critical $U$-dependent density [11]. The Gutzwiller variational approximation has been applied [12], even for large $U$, yielding results qualitatively similar to the Hartree–Fock approximation. However, for large $U$, a ferromagnetic domain appears only if the density is larger than some critical value. The same behaviour holds when the stability of the ferromagnetic state is investigated on variational grounds [13–17] or in the high-temperature expansion [18], whereas several authors [19, 20] even questioned the appearance of a ferromagnetic domain at all. Attempts

† Present address: Max-Planck-Institut für Festkörperforschung, Heisenbergstrasse 1, D-7000 Stuttgart 80, Federal Republic of Germany.

0953-8984/93/274847+08$07.50 

to partially satisfy both antiferromagnetic and ferromagnetic tendencies by allowing for other translational-invariant magnetic states which represent compromises between both, such as spiral, canted, ferrimagnetic and linearly polarized spin-density waves, have been investigated in several frameworks. Shraiman and Siggia [21] demonstrated the existence of interaction terms favouring spiral order in an effective classical field theory of doped antiferromagnets. The effect of quantum fluctuations in spiral phases has been considered in [22], and a double spiral structure has been identified as the lowest-energy state there, and both in the Gutzwiller variational approximation [23] and in the Hartree–Fock approximation [6, 7, 9], a spiral magnetic solution is found to be lower in energy than the antiferromagnetic state for any finite doping. Recently more complex solutions of the Hartree–Fock theory have been studied, such as domain-wall structures of various kinds [11, 24–26].

In the Kotliar and Ruckenstein slave-boson technique [27] the Gutzwiller approximation appears as a saddle-point approximation of this field theoretical representation of the Hubbard model. In the latter the contribution of the thermal fluctuations has been calculated [28] and turned out to be incomplete as this representation, even though exact, is not manifestly spin rotation invariant. Spin-rotation-invariant [29] and spin- and charge-rotation-invariant [30] formulations have been proposed, and the first was used to calculate correlation functions [31] and the spin fluctuation contribution to the specific heat [32]. Moreover the instability line of the paramagnetic state with respect to arbitrary incommensurate spin ordering has been determined [33] and did not exhibit an instability towards the ferromagnetic state. Comparisons of the ground-state energy with quantum Monte Carlo simulations, including antiferromagnetic ordering [34] and spiral states [35], or with exact diagonalization data [36] have been made and yield excellent agreement, and such spiral states have been investigated independently by Arrigoni and Strinnati [37]. In this paper we determine the domain of the phase diagram of the Hubbard model on the square lattice where the ferromagnetism takes place, in the spin-rotation-invariant slave-boson theory when spiral states are allowed. In addition we determine analytically the critical density $n_c(U = \infty)$ on the $d$-dimensional hyper-cubic lattice at which the fully polarized ferromagnetic state is degenerate with the paramagnetic state as obtained in the saddle-point approximation of the slave-boson approach.

## 2. Magnetic phase diagram

We consider the Hubbard model for electrons on the square lattice:

$$H = \sum_{\langle i,j\rangle,\sigma} t_{i,j} c^{+}_{i,\sigma} c_{j,\sigma} + U \sum_{i} n_{i,\uparrow} n_{i,\downarrow} \tag{1}$$

with nearest-neighbour hopping matrix elements $t_{i,j} = -t$, and the sum over the neighbours taken in such a way that the bare band width is $8t$. As the expression for the free energy in the slave-boson approach when spiral states are allowed has been given in [36], we simply remind the reader that within the saddle-point approximation, the expectation value of the number of respectively empty, singly occupied and doubly occupied sites is denoted by $e^2$, $p_0^2 + p^2$, and $d^2$, and the site-dependent averaged magnetization $m_i$ by $2p_0p_i$. Allowing for spiral states implies

$$p_i = p\hat{n}_i \tag{2}$$

where the unit vector $\hat{n}_i$ forms a spiral structure, e.g.

$$\hat{n}_i = (\cos\phi_i, \sin\phi_i, 0) \tag{3}$$

with the site-dependent rotation angle

$$\phi_i = \boldsymbol{Q} \cdot \boldsymbol{R}_i \qquad \boldsymbol{R}_i = a(n_1, n_2). \tag{4}$$

Using

$$z_\pm = B_+ L_+ R_- \pm B_- L_- R_+ \tag{5}$$

where

$$L_\pm = [1 - d^2 - \tfrac{1}{2}(p_0 \pm p)^2]^{-1/2} \tag{6}$$

$$R_\pm = [1 - e^2 - \tfrac{1}{2}(p_0 \pm p)^2]^{-1/2} \tag{7}$$

$$B_\pm = (1/2\sqrt{2})[p_0(e+d) \pm p(e-d)] \tag{8}$$

one then obtains two quasi-particle bands with the dispersion relation

$$E_{k,\nu} = \tfrac{1}{2}(z_+^2 + z_-^2)(t_k + t_{k+Q}) + \beta_0 - \mu + \nu\tfrac{1}{2}\{(z_+^2 - z_-^2)^2(t_k - t_{k+Q})^2 + 4[z_+ z_-(t_k + t_{k+Q}) + \beta]^2\}^{1/2} \qquad \nu = \pm 1. \tag{9}$$

The mean-field free energy follows as

$$F = -T\sum_{k,\nu} \ln[1 + \exp(-E_{k,\nu}/T)] + Ud^2 + \alpha(e^2 + d^2 + p_0^2 + p^2 - 1) - \beta_0(2d^2 + p_0^2 + p^2) - 2\beta p p_0 \tag{10}$$

where $\alpha$, $\beta$ and $\beta_0$ are the Lagrange multipliers enforcing the constraints. One thus has to solve the saddle-point equations with respect to the parameters $e$, $p_0$, $p$, $d$, $\alpha$, $\beta$, $\beta_0$, and $\boldsymbol{Q}$ to obtain $F$. (Actually one parameter, say $d$, would be complex [30, 38] with a phase $\varphi$. However this additional parameter plays no role as $\partial F/\partial\varphi$ is proportional to $\sin\varphi$ and the saddle-point equations deliver $\varphi = 0$.) Alternatively one can first remove the $d$ field by taking the constraint enforced by the Lagrange multiplier $\alpha$ into consideration, then define a function $g(e, p_0, p, \boldsymbol{Q})$ as the maximum of $F$ with respect to $\beta_0$ and $\beta$, and then minimize $g$ with respect to the parameters $e$, $p_0$, $p$ and $\boldsymbol{Q}$. The saddle point of $F$ is reached when the minimum of $g$ is obtained. It turned out that this procedure was much easier to implement in the computer than that which consists of directly solving the saddle-point equations. Moreover we achieved this procedure on the $98 \times 98$ lattice at $T = t/100$. The systematic error following from finite-size effects is then of the order of $10^{-4}$. In addition we would like to stress that we are indeed looking for a saddle point of $F$, as having non-vanishing Lagrange multipliers only corresponds to a shift of the integration contour for the constraint fields.

Useful analytical results can be obtained by noticing that the Lagrange multiplier $|\beta|$ is growing like $U/2$ at half filling for large $U$. It thus provides a small parameter $(t_k/\beta)$ allowing for an expansion of the quasi-particle dispersion relation in powers of $(t/U)^2$, and thus allowing for an analytical minimization of the free energy. As this procedure leads to a rather lengthy calculation [39], we shall only quote the outcome and compare it with the numerical results.

In figure 1 we display the $x$ component of the spiral wave-vector as function of the hole doping for several values of the interaction strength. It turns out that spiral wave-vectors which minimize the energy belong to three different families: either $\boldsymbol{Q} = q_x(1, 1)$, hereafter denoted by $(q, q)$, or $\boldsymbol{Q} = (q_x, \pi)$, hereafter denoted by $(q, \pi)$, or $\boldsymbol{Q} = (0, q_x)$, hereafter denoted by $(0, q)$. At half filling we obtain the AF state as ground state. For $U/t = 60$, the spiral wave-vector is lying on the diagonal of the first Brillouin zone for small doping. Even

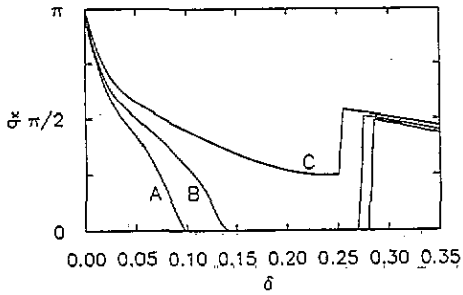


**Figure 1.** $x$ component of the spiral wave-vector as a function of doping for $U/t = 60$ (curve C), 80 (curve B), and 100 (curve A). The jumps indicate the transition from the $(q, q)$ spiral state and the ferromagnetic state, respectively, to the $(q, \pi)$ spiral state.

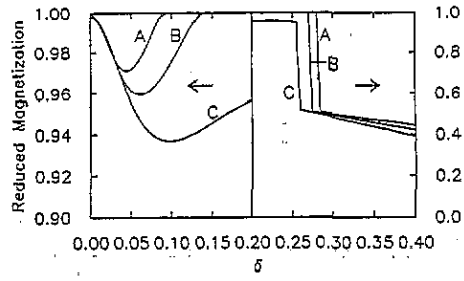


**Figure 2.** Reduced magnetization $m_r$ (see text) as a function of doping for $U/t = 60$ (curve C), 80 (curve B), and 100 (curve A). The jumps indicate the transition from the $(q, q)$ spiral state and the ferromagnetic state, respectively, to the $(q, \pi)$ spiral state.

though the difference in energy between the $(q, q)$ and the $(q, \pi)$ spiral states, and even between both and the antiferromagnetic state, are quite tiny, particularly close to half filling, the $(q, q)$ state is lowest in energy. The gain in energy with respect to the antiferromagnetic state is found to be $U\delta^2$ in the $(q, q)$ state, and only $U\delta^2/2$ in the $(q, \pi)$ state. In both states one obtains

$$q_x \simeq \pi - \delta U/t \qquad \text{if } 8(t/U)^2 \ll \delta \ll (2t/U)^{4/3}. \tag{11}$$

Upon a further increase of the doping the system undergoes a first-order transition to another spiral phase, namely the $(q, \pi)$ phase. However, there is clearly no indication of ferromagnetism and thus no qualitative difference with the smaller-$U$ domain as discussed in detail in [36], apart from the appearance of the additional $(0, q)$ phase in the very close vicinity of the spiral–paramagnetic transition. The transition from the $(q, \pi)$ phase to the $(0, q)$ phase is smooth, i.e. second order, and is only signalled by the fact that $\boldsymbol{Q}$ changes from one type to the other as there is a value of the doping such that the collinear state $(\boldsymbol{Q} = (\pi, 0))$ is lowest in energy. For larger interaction strength, i.e. $U/t$=80 or 100, one clearly sees in figure 1 that in the $(q, q)$ phase $q_x$ goes smoothly from $\pi$ at half filling down to 0 at some critical doping $\delta_c$, thus signalling the occurrence of a ferromagnetic domain. From the numerical data $q_x$ is seen to vanish at the transition as $(\delta_c - \delta)^\nu$ with $\nu \simeq \frac{2}{3}$ or a little smaller.

In order to know whether or not we obtain the fully polarized ferromagnetic state (FPFS) we show in figure 2 the reduced magnetization as a function of the hole doping for the same values of $U$ as in figure 1; the reduced magnetization $m_r$ is defined as $m/n$, and thus takes the value unity in the FPFS. At half filling and for $U \gg t$, $m_r$ is given by

$$m_r \simeq 1 - 8(t/U)^2 - 104(t/U)^4. \tag{12}$$

Upon doping $m_r$ is first decreased as

$$m_r \simeq 1 - 8(t/U)^2 - U^2\delta^3/2t^2 + 2\delta^2 \qquad \text{if } 8(t/U)^2 \ll \delta \ll (2t/U)^{4/3} \tag{13}$$

but thus increases again upon doping to reach unity exactly when $q_x$ goes to zero, thus yielding no evidence for a non-fully polarized ferromagnetic state.

Returning to figure 1, a further increase of the doping leads to a first-order transition from the FPFS to the $(q, \pi)$ spiral phase, then to the $(0, q)$ spiral phase and finally to the paramagnetic state. Even though $m_r$ is still quite large in the $(q, \pi)$ phase, $m_r \simeq 0.5$ for $\delta \simeq$ 30–40%, the gain in energy with respect to the paramagnetic state is very small,

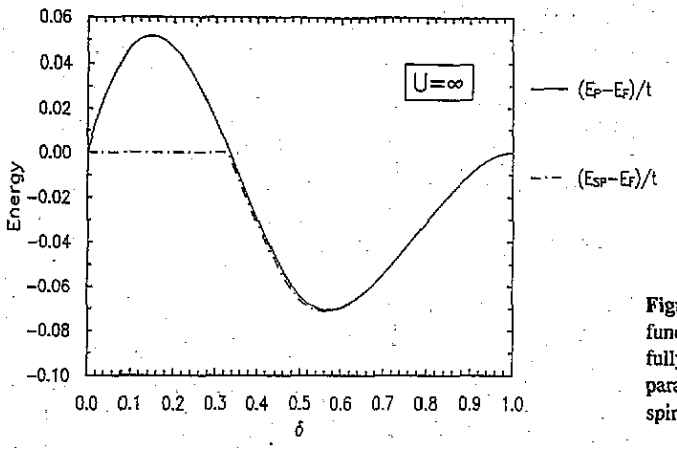


**Figure 3.** Ground-state energy as a function of the doping relative to the fully polarized ferromagnetic state in the paramagnetic state (full curve) and in the spiral state (chain curve) for $U = \infty$.

but at least one order of magnitude larger than the systematic error following from our numerical procedure. This is exemplified in figure 3 where we display the ground-state energy as a function of the hole doping for an infinite interaction strength relative to the FPFS ground-state energy for both paramagnetic and spiral states. One clearly sees that the gain in energy is substantial only where we find the FPFS as lowest in energy. Moreover the spiral–paramagnetic phase boundary as obtained from this calculation and from a diverging $q$-dependent spin susceptibility [33] are in very good agreement.

Some insight into the stability of the ferromagnetic and spiral states can be gained by looking at the behaviour of the Lagrange multiplier $\beta$ which governs both the band width and the magnetic gap. At half filling $|\beta|$ is growing as

$$\beta = -U/2 + 12t^2/U \tag{14}$$

for $U \gg t$, thus yielding a band width proportional to $J$, where $J$ is the exchange coupling, and a magnetic gap of order $U$. But upon doping, $\beta$ is considerably decreased as

$$\beta = -U/2 + 12t^2/U + U^5\delta^3/32t^4 \qquad \text{if } 8(t/U)^2 \ll \delta \ll (2t/U)^{4/3} \tag{15}$$

to be of order $t$ for $\delta \simeq t/U$ (in contrast to the Hartree–Fock approximation where the magnetic gap is given to a good approximation by $Um$ [9]). Thus, upon doping, the band width goes from $4J$ at half filling up to $\sim 4z_0^2 t$ for $\delta \geqslant t/U$, where $z_0^2$ stands as a mass renormalization factor, which is close to that obtained in the paramagnetic state.

In figure 4 we display $\Delta$, which is defined as the difference in energy between the bottom of the upper magnetic sub-band and the Fermi energy, as a function of the doping for several interaction strengths. (Here we set $\Delta$ to 0 in the FPFS as it is undetermined.) It clearly appears that the upper magnetic sub-band does not contribute to the mean-field free energy even though the two bands may overlap. However both magnetic sub-bands are sufficiently close to one another at the mean-field level that one cannot exclude that both would contribute in a more refined calculation, leading for instance to a reduced magnetization, apart from the close vicinity of half filling, where they definitively separate, the upper one merging with the upper Hubbard band which is absent from this calculation.

Our results are summarized in the phase diagram in figure 5. It consists of six phases. At half filling, and half filling only, the ground state is the antiferromagnetic one. Upon doping it is unstable towards the $(q, q)$ spiral phase. In this phase the compressibility is changing from negative, for very small doping, to positive, thus leading to a thermodynamically stable phase. However, the phase-separated domain is seen to be quite small, much smaller than in the Hartree–Fock approximation [10]. For sufficiently large $U$, i.e. $U/t > 66$, the spiral

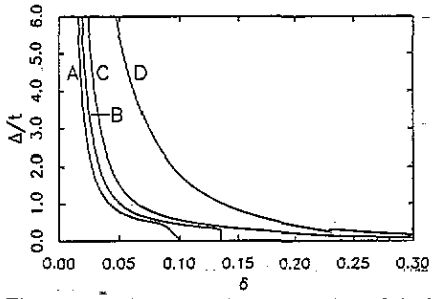


**Figure 4.** $\Delta/t$ (see text) as a function of doping for $U/t = 20$ (curve D), 60 (curve C), 80 (curve B), and 100 (curve A). The jumps indicate the transition from the $(q, q)$ spiral state and the ferromagnetic state, respectively, to the $(q, \pi)$ spiral state.

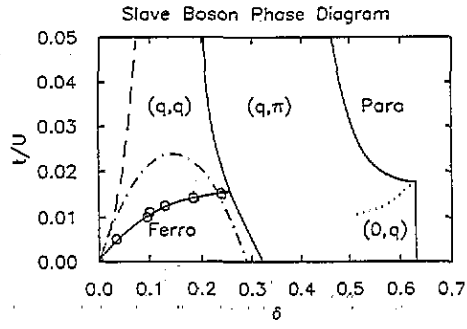


**Figure 5.** Phase diagram. Full curves: phases boundaries in the slave-boson mean-field theory. Broken curves: zero-compressibility line, separating single-phase and phase separated states. Dotted curve: phase boundary curve between the $(q, \pi)$ and the $(0, q)$ states; this is mainly meant as a guide for the eye, owing to the difficulty in determining it. Chain curve: instability curve of the ferromagnetic state as extracted from [13]. (In particular the phase boundary line between the ferromagnetic and the spiral states follows from the numerical data which are represented by the circles.)

wave-vector is moving along the diagonal of the Brillouin zone up to the centre. In that case the spiral phase plays its role of compromise between the antiferromagnetic and the ferromagnetic phases. For larger doping one obtains a $(q, \pi)$ phase, possibly a $(0, q)$ phase, and finally, for even larger doping, the paramagnetic phase. The transition from the $(q, q)$ phase, or the ferromagnetic one, to the $(q, \pi)$ phase is first order; the others are second order. We were able to determine the transition line between the $(q, \pi)$ and the $(0, q)$ phases only for $U/t \leqslant 100$. For larger $U$ the difference in energy between the two phases is smaller than the systematic error originating from finite-size effects. The ferromagnetic domain as obtained from this calculation is in good agreement with that obtained by von der Linden and Edwards [13]. In particular for $U = \infty$, the ferromagnetic state is unstable for $\delta_c > 0.33$, while [13] gives $\delta_c = 0.29$, Gutzwiller wave-function calculations allowing for spiral states give $\delta_c = 0.375$ [23], and high-temperature expansion yields $\delta_c = 0.27$ [18].

Actually $\delta_c$ as obtained from our calculation differs only slightly from that obtained within the usual Gutzwiller approximation, i.e. with paramagnetic states only. In that case we can determine, at $U = \infty$, the critical hole concentration at which the ferromagnetic and the paramagnetic states are degenerate. On the $d$-dimensional hyper-cubic lattice one has to solve

$$F_P(\delta_c) = F_F(\delta_c) \tag{16}$$

where the free energy in the paramagnetic state is given by

$$F_P = 2z_0^2 \int_{-\infty}^{\mu_P} d\epsilon\, \epsilon\rho(\epsilon) \tag{17}$$

where $\rho(\epsilon)$ is the density of states per spin and, at $U = \infty$, the mass renormalization factor becomes

$$z_0^2 = 2\delta/(1+\delta) \tag{18}$$

and

$$F_F = \int_{-\infty}^{\mu_F} d\epsilon\, \epsilon\rho(\epsilon). \tag{19}$$

(16) is obviously solved provided $z_0^2 = \frac{1}{2}$ and $\mu_P = -\mu_F$ as $\rho(\epsilon)$ is an even function of $\epsilon$. The second condition implies

$$2n(\mu_P) = n(\mu_F) = 1 - n(\mu_P) \tag{20}$$

yielding $2n(\mu_P) = \frac{2}{3}$ in which case $z_0^2(\delta_c) = \frac{1}{2}$. Thus (16) is solved at the critical hole concentration of $\frac{1}{3}$, independently of the dimension of the system which is in agreement with its numerical determination [33, 40]. In this light the limit of infinite dimensions [41] appears somewhat special, as it is the only case allowing for a finite value of $d$ for infinite $U$. Actually this argument is valid for any bipartite lattice, as the only requirement is an even density of states, but only applies provided that the paramagnetic state is not unstable towards another state for a larger density of holes.

## 3. Conclusion

We applied the slave-boson mean-field approach, first introduced by Kotliar and Ruckenstein [27], and then made spin rotation invariant [29, 30], to spiral magnetic states in the Hubbard model. The phase diagram is found to consist of six regions: at half filling the ground state is antiferromagnetic. Upon doping it is immediately unstable towards the $(q, q)$ spiral phase. If the interaction strength is large enough ($U/t > 66$) the spiral wave-vector will reach the centre of the first Brillouin zone and we obtain a ferromagnetic region. Increasing the doping further leads to a first-order phase transition from either the ferromagnetic (if $U/t > 66$) or the $(q, q)$ spiral state (if $U/t < 66$) to the $(q, \pi)$ spiral state. A further increase of the doping drives the system through a second-order phase transition to the paramagnetic state if $U/t < 57$, or to the $(0, q)$ spiral state and finally to the paramagnetic through two second-order phase transitions if $U/t > 57$. The phase boundary of the paramagnetic state is in agreement with that determined in [33]. We compare the ferromagnetic domain with that obtained in other frameworks [18, 23] and particularly with [13] and they are all seen to be in qualitative agreement. Moreover, for large $U$, it turns out that the magnetic gap is very strongly affected by doping and is even seen to vanish for rather small doping ($\sim 10\%$). As a consequence one obtains a transfer of spectral weight from the upper to the lower band upon doping. We put a particular emphasis on the first-order phase transition from the ferromagnetic and paramagnetic states at $U = \infty$ on the $d$-dimensional hyper-cubic lattice and find a $d$-independent critical hole doping of $\frac{1}{3}$. However a more accurate description of the upper Hubbard band, including fluctuations, is highly desirable. Work along this line is in progress.

## Acknowledgments

This work has been supported by the Deutsche Forschungsgemeinschaft under SFB 195. One of us (RF) thanks the Fonds National Suisse de la Recherche Scientifique for financial support and BM thanks the Forschungsschwerpunkt Supraleitung im Landesforschungsförderungsprogramm Baden-Württembergs for financial support. We thank Professor P Wölfle for many enlightening discussions and Dr M Dzierzawa for many interesting discussions.

## References


[1] Anderson P W 1987 *Science* **235** 1196
[2] Mattis D C 1981 *The Theory of Magnetism I (Springer Ser. Solid State Sci. 17)* (Berlin: Springer)
[3] Liang S, Douçot B and Anderson P W 1988 *Phys. Rev. Lett.* **61** 365
Trivedi N and Ceperley D 1989 *Phys. Rev.* B **40** 2737
[4] Barbieri A, Riera J A and Young A P 1990 *Phys. Rev.* B **41** 11 697
[5] Penn D R 1966 *Phys. Rev.* **142** 350
Cyrot M 1972 *J. Physique* **33** 125
[6] Yoshioka D 1989 *J. Phys. Soc. Japan* **58** 1516
[7] Jayaprakash C, Krishnamurthy H R and Sarker S 1989 *Phys. Rev.* B **40** 2610
Sarker S, Jayaprakash C, Krishnamurthy H R and Wenzel W 1991 *Phys. Rev.* B **43** 8775
[8] Schulz H 1990 *Phys. Rev. Lett.* **65** 2462
[9] Dzierzawa M 1992 *Z. Phys.* B **86** 49
[10] John S, Voruganti P and Goff W 1991 *Phys. Rev.* B **43** 13 365
[11] Schulz H 1990 *Phys. Rev. Lett.* **64** 1445
[12] Metzner W and Vollhardt D 1989 *Phys. Rev. Lett.* **62** 324
Metzner W 1989 *Z. Phys.* B **77** 253
[13] von der Linden W and Edwards D W 1991 *J. Phys.: Condens. Matter* **3** 4917
[14] Ruckenstein A E and Schmitt-Rink S 1989 *Int. J. Mod. Phys.* B **3** 1809
[15] Shastry B S, Krishnamurthy H R and Anderson P W 1990 *Phys. Rev.* B **41** 2375
[16] Basile A G and Elser V 1990 *Phys. Rev.* B **41** 4842
[17] Kopp Th, Ruckenstein A and Schmitt-Rink S 1990 *Phys. Rev.* B **42** 6850
[18] Putikka W O, Luchini M U and Rice T M 1992 *Phys. Rev. Lett.* **68** 53
[19] Chen L, Bourbonnais C, Li T C and Tremblay A-M S 1991 *Phys. Rev. Lett.* **66** 369
[20] Douçot B and Rammal R 1989 *Int. J. Mod. Phys.* B **3** 1775
[21] Shraiman B and Siggia E 1990 *Phys. Rev. Lett.* **62** 1564
[22] Kane C L, Lee P A, Ng T K, Chakravarty B and Read N 1990 *Phys. Rev.* B **41** 2653
[23] Dzierzawa M and Frésard R Z. *Phys.* B at press
[24] Poilblanc D and Rice T M 1989 *Phys. Rev.* B **39** 9749
[25] Bishop A R, Guinea F, Lomdahl P S, Louis E and Vergés J A 1991 *Europhys. Lett.* **14** 157
[26] Machida K 1989 *Physica* C **158** 192
Kato M, Machida K, Nakanishi H and Fujita M 1990 *J. Phys. Soc. Japan* **59** 1047
[27] Kotliar G and Ruckenstein A 1986 *Phys. Rev. Lett.* **57** 1362
[28] Rasul J W and Li T C 1988 *J. Phys. C: Solid State Phys.* **21** 5119
Li T C and Rasul J W 1989 *Phys. Rev.* B **39** 4630
Rasul J W, Li T C and Beck H 1989 *Phys. Rev.* B **39** 4191
[29] Li T, Wölfle P and Hirschfeld P 1990 *Phys. Rev.* B **40** 6817
[30] Frésard R and Wölfle P 1992 *Proc. Adriatico Res. Conf. Miniworkshop on Strongly Correlated Electron Systems III; Int. J. Mod. Phys.* B **6** 685; Erratum 1992 **6** 3087
[31] Li T C, Sun Y S and Wölfle P 1991 *Z. Phys.* B **82** 369
[32] Wölfle P and Li T C 1990 *Z. Phys.* B **78** 45
[33] Doll K, Dzierzawa M, Frésard R and Wölfle P 1993 *Z. Phys.* B **90** 297
[34] Lilly L, Muramatsu A and Hanke W 1990 *Phys. Rev. Lett.* **65** 1379
[35] Frésard R, Dzierzawa M and Wölfle P 1991 *Europhys. Lett.* **15** 325
[36] Frésard R and Wölfle P 1992 *J. Phys.: Condens. Matter* **4** 3625; *Proc. Phys. Two Dimensions Conf. (Neuchâtel, 1991); Helv. Phys. Acta.* **65** 423
[37] Arrigoni E and Strinnati G C 1991 *Phys. Rev.* B **44** 7455
[38] Jolicœur Th and Le Guillou J C 1991 *Phys. Rev.* B **44** 2403
[39] Doll K 1992 *Diploma Thesis* University Karlsruhe
[40] Deeg M, Fehske H and Büttner H 1992 *Z. Phys.* B **88** 283
[41] Fazekas P, Menge B and Müller-Hartmann E 1990 *Z. Phys.* B **78** 69